Gas propagation following a sudden loss of vacuum in a pipe cooled by He I and He II.

Nathaniel Garceau, Shiran Bao, Wei Guo

Cryogenics Group, National High Magnetic Field Laboratory – Tallahassee FL 32310

FAMU-FSU College of Engineering, Florida State University – Tallahassee FL 32310

Abstract

Vacuum break in particle accelerators is a major concern due to risks associated with personnel and extensive equipment damage. Continuing research in our lab focuses on the sudden loss of vacuum in the liquid helium cooled beam-line tubes of superconducting particle accelerators. In our previous research, we studied nitrogen gas propagation in a uniform tube system immersed in both normal helium (He I) and superfluid helium (He II). It was observed that He II has a stronger effect in slowing down the gas propagation compared to He I, but this effect was largely due to the variation of the point where condensation and deposition of the nitrogen gas on the tube inner wall [4]. Here, we discuss our modifications to the tube system that now allow us to accurately control the starting location of gas condensation in both the He I and He II experiments. Systematic studies of gas propagation were conducted using this new tube system by varying the nitrogen mass flow rate at the tube inlet. Finally there is a brief overview of the preliminary model which captured the main physics which occur after a vacuum break in the simplified beam tube.

Introduction

Particle accelerator systems are cryogenic systems are composed of multiple segments called cryomodules which contain SRF niobium cavities, liquid baths of He II, sensors and other machinery. Cryomodules contain two vacuum spaces. The first vacuum space is the insulation space for the He II bath which immerses the niobium cavity. The second vacuum space is in the center niobium beam tube where the accelerated particles travel. The second vacuum space is an interconnected void between all cryomodules of the system. If there is a sudden rupture of this second vacuum space then there is potential that the entire system could become affected.

Previous research at the National High Magnetic Field Lab attempted to quantify and model the propagation of the gas front in the beam tube in the event of a catastrophic loss of vacuum [1-3]. To simulate the air propagation in the system, a pipe was immersed in liquid helium (LHe) and nitrogen was allowed to rush in. The propagation in the cryogenic system is order of magnitudes slower than at room temperature due to the air freezing to the tube walls. Illustration of a vacuum break in a tube system is illustrated in figure 1 below.

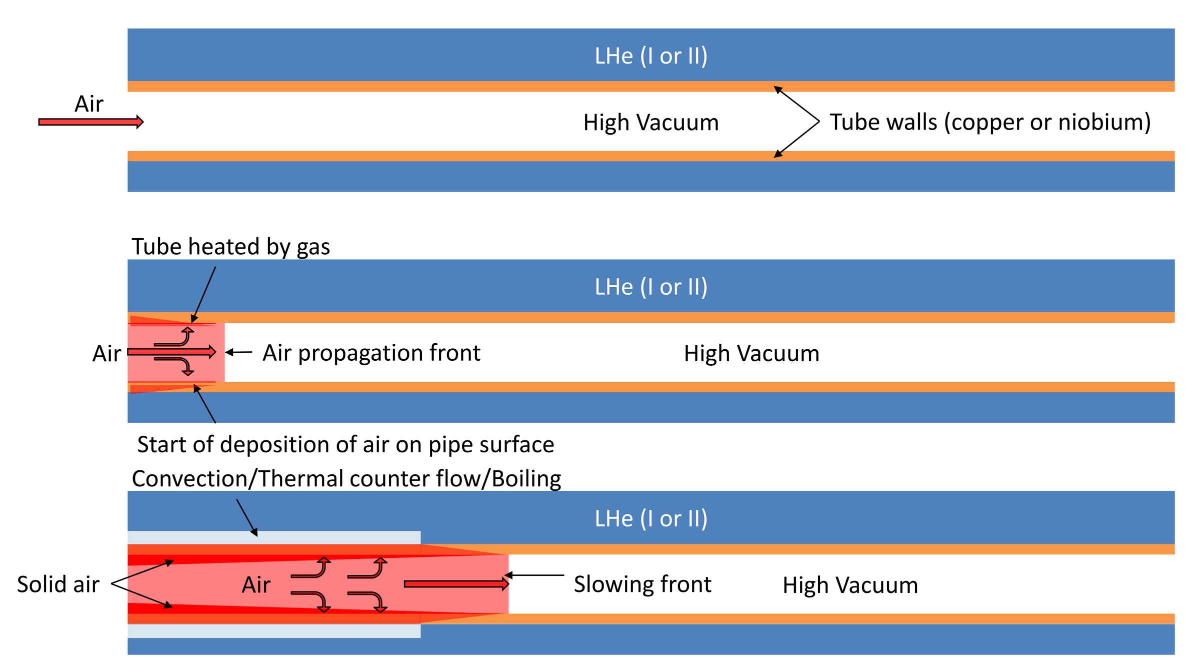

Figure 1. Air propagation following a vacuum tube in a tube surrounded by liquid helium.

Experiment

Equipment and instrumentation

- 7-8 Epoxy encapsulated Lakeshore Cernox diodes
- 4 DT9824 ISO-Channel Data Acquisition Boxes (4800 Hz)
- Edwards D145 cold cathode gague (range 10^{-3} to 10^{-7} torr)
- MKS Batatron 626 (1000 Torr gauge)
- Venturi tube to choke flow providing constant mass flow

Helical tube system dimensions	
Pipe length (m)	5.75
Pipe inner diameter (mm)	25.4
Wall thickness (mm)	1.25
Coil diameter (mm)	229
Coil pitch (mm)	51
Number of temperature sensors	8
Distance between sensors (mm)	719
Nitrogen reservoir tank (L)	227

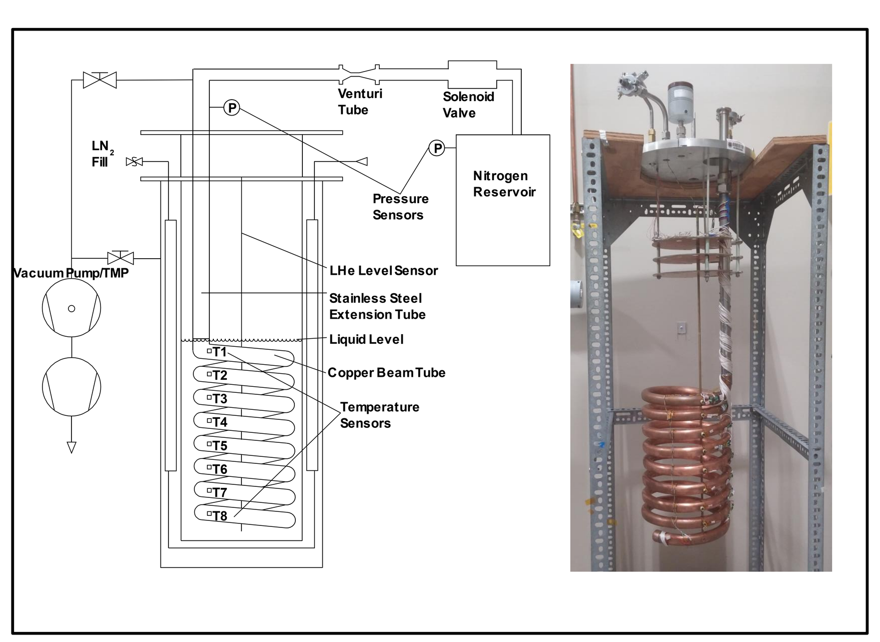

Figure 2. Uninsulated Helical tube system schematic and image.

Upgraded Insulated System

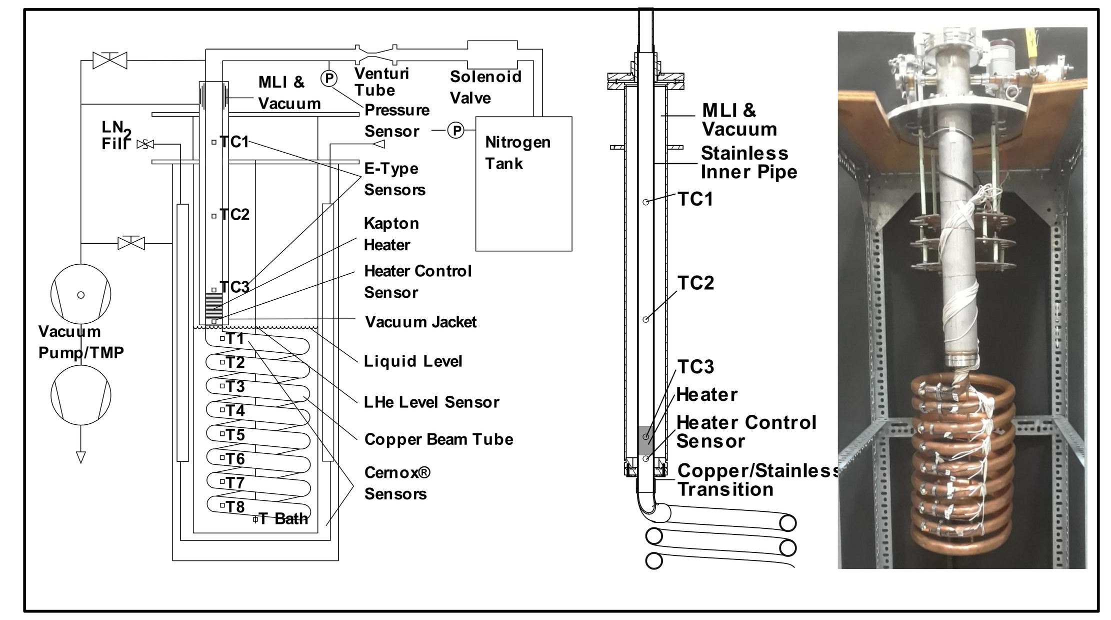

Figure 3. Insulated Helical tube system schematic, CAD drawing and image.

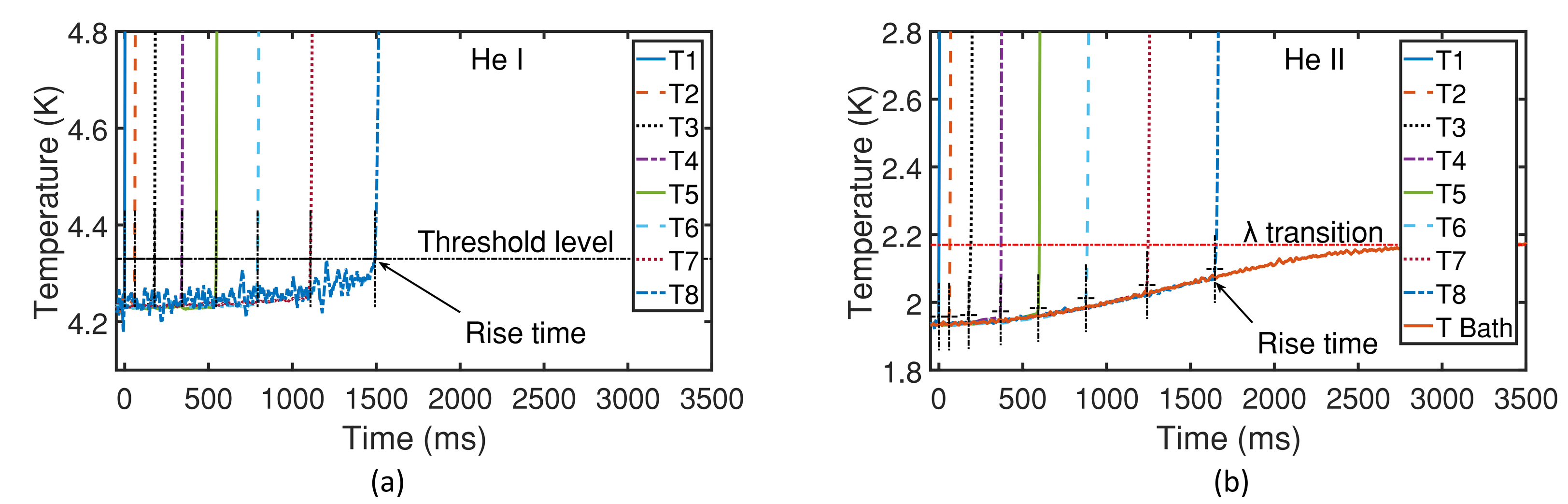

Figure 4. Smoothed temperature over time data for He I (a) and He II (b) experiments. Threshold level is indicated by a dashed horizontal line. Threshold level is used for determining the rise time of each sensor (short vertical lines).

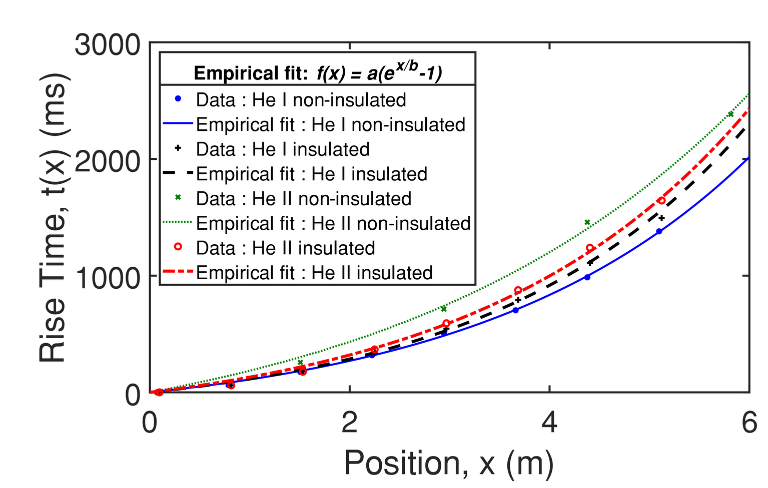

Figure 5. Risetime position comparison of He I and He II experiments for both insulated and non-insulated cases.

Note: Thermocouple temperatures for both He I and He II insulated system were 250 K, 210 K and 150 K, which was well above the critical point of nitrogen. For the non-insulated experiments for the He II the upper temperature profile was 60 K, 15 K and 3 K [4].

Data confirms that temperature profile above the liquid level will affect propagation slowing.

Mass Flow Variations

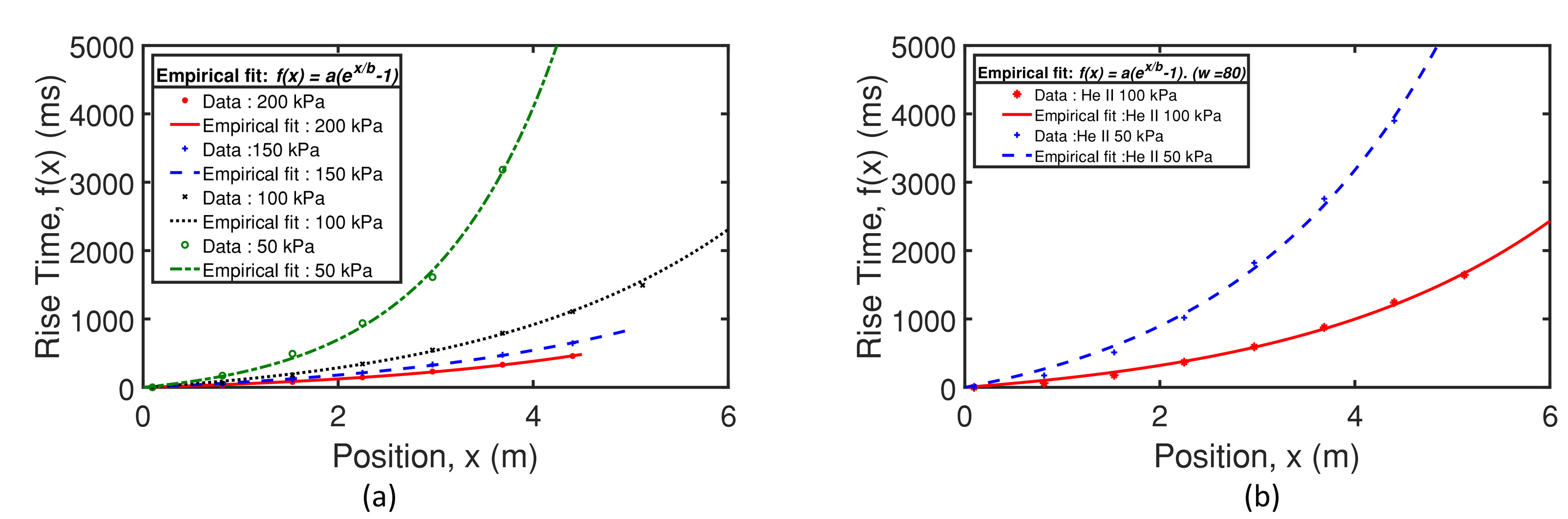

Figure 6. Rse time vs position comparison for different mass flow rates for He I (a) and He II (b).

Mass flow varied by changing pressure of buffer tank. 50 kPa, 100 kPa, 150 kPa, and 200 kPa correspond to an average mass flow of 9.8 g/s, 18.3 g/s, 26.1 g/s and 35.2 g/s. Freeze out seen in 50 kPa cases between last two sensors.

Preliminary Numerical Model

Conservation of Energy

$$\frac{\partial}{\partial t}\left[\rho\left(\varepsilon+\frac{1}{2}v^2\right)\right]+\frac{\partial}{\partial x}\left[\rho v\left(\varepsilon+\frac{1}{2}v^2+\frac{P}{\rho}\right)\right]=-\frac{4}{D_1}\dot{m}_c\left(\varepsilon+\frac{1}{2}v^2+\frac{P}{\rho}\right)-\frac{4}{D_1{}^2}Nu\cdot k\left(T_g-T_s\right)$$

Conservation of Mass

$$\frac{\partial\rho}{\partial t}+\frac{\partial}{\partial x}(\rho v)=-\frac{4}{D_1}\dot{m}_c$$

Conservation of Momentum

$$\frac{\partial}{\partial t}(\rho v)+\frac{\partial}{\partial x}(\rho v^2)=-\frac{\partial P}{\partial x}-\frac{4}{D_1}\dot{m}_c v$$

Radial heat transfer

$$\rho_w S_w\frac{D_2^2-D_1^2}{4D_1}\frac{\partial T_s}{\partial t}=q-q_{he}\frac{D_2}{D_1}$$

Heat flux through wall

$$q=\dot{m}_c\left[\frac{1}{2}v^2+\hat{h}(T_g,P)-\hat{h}(T_s,P)\right]-\frac{Nu\cdot k}{D_1}\left(T_g-T_s\right)$$

Sticking coefficient

$$\dot{m}_c=\dot{m}_o\cdot C(T_g,T_s,P)=\rho_g\sqrt{\frac{RT_g}{2\pi M_g}}\cdot C(T_g,T_s,P)$$

Ideal Gas (Nitrogen)

$$PM=\rho RT_g$$

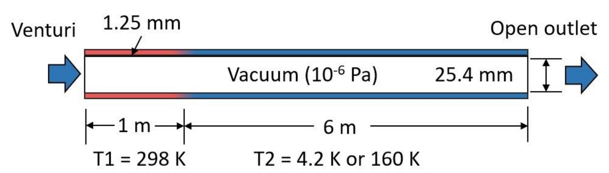

Figure 7. Schematic diagram showing the tube geometry and initial conditions used in preliminary simulation

Variable	Description
ρ	Gas bulk density
ρ	Gas density at the wall surface
v	Gas velocity
Pe	Gas equilibrium pressure
Ps	Gas saturated vapour pressure at surface temperature
T_g	Gas Temperature
M	Gas molar mass
$\dot{h}_g$	Gas Enthalpy
$\dot{h}_s$	Solid nitrogen enthalpy
ε	Internal energy of the ideal gas
C	Effective sticking coefficient
S_w	Specific heat of the wall material
R	Ideal gas constant
Nu	Nusselt number
$\dot{m}_c$	Condensation mass flow rate
$\dot{m}_o$	Mass flow rate toward tube wall
x	Position along the tube
D_1	Tube inner diameter
D_2	Tube outer diameter
T_s	Tube wall surface temperature
K	Tube wall thermal conductivity
q	Heat flux into the wall
q_{he}	Heat flux into the liquid helium

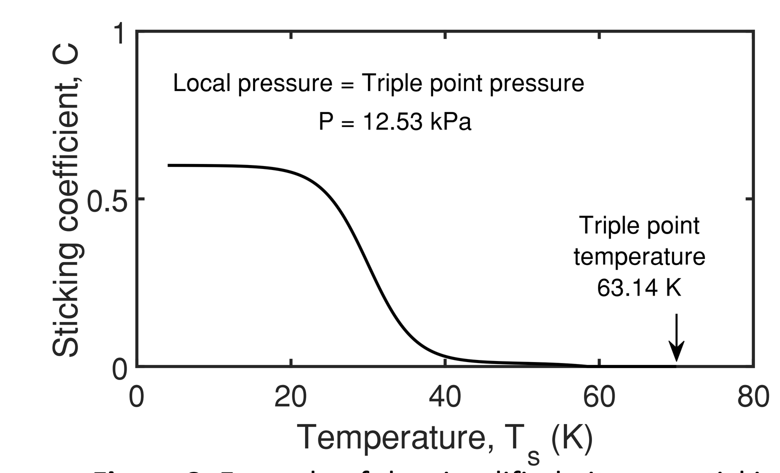

Figure 8. Example of the simplified nitrogen sticking coefficient model used in the preliminary simulation.

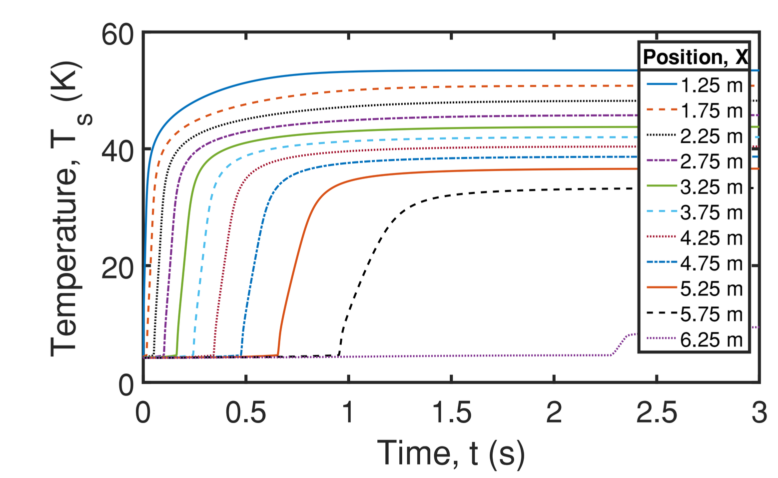

Figure 9. Simulated wall temperature profiles for system

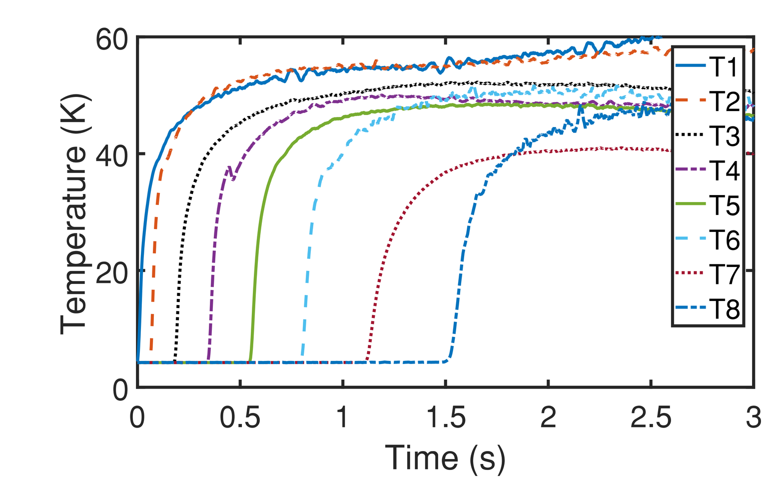

Figure 10. Experimental wall temperature profiles for He I 100 kPa.

Conclusion

- System vacuum MLI insulation reduced differences seen in the He I and He II experiments significantly by mitigating the convective cooling effects seen during He II evaporative cooling phase.
- Stronger propagation slowing effect seen at lower mass flow rates. Freeze out occurring before sensor T7 in 50 kPa-9.8 g/s run.
- Preliminary simulation captures the main physics of the gas flow. Model expansion needs to include building frost layer and better representation of the sticking coefficient model. Comparison of the model to different mass flow rates to be conducted in future.

Acknowledgments

This work is supported by U.S. Department of Energy grant DE-FG02-96ER40952. The experiments were conducted at the National High Magnetic Field Laboratory, which is supported by NSF DMR-1157490 and the State of Florida.

References

[1] R. Dhuley, S.W. Van Sciver. *Propagation of nitrogen gas in a liquid heium cooled vacuum tube following sudden vacuum loss – Part 1: Experimental investigations and analytical modeling.* J. of Heat and Mass Transfer, V96, 2016, pp 573-581

[2] R. Dhuley, S.W. Van Sciver. *Propagation of nitrogen gas in a liquid heium cooled vacuum tube following sudden vacuum loss – Part 2: Analysis of the propagation speed.* J. of Heat and Mass Transfer, V98, 2016 pp 728-737

[3] R. Dhuley, S.W. Van Sciver. Epoxy encapsulation of Cernox SD thermometer for measuring the temperature of surface in liquid helium. Cryogenics, V77, 2016, pp 49-52

[4] N. Garceau, S. Bao, W. Guo *Heat and mass transfer during a sudden loss of vacuum in a liquid helium cooled tube – Part I: Interpretation of experimental observations.* J of Heat and Mass Transfer, V 129, 2019 pp 1144-1150